

ON THE MASS DEPENDENCE OF THE INNER SLOPES OF DARK MATTER DENSITY PROFILES

A. Del Popolo^{1,2}

¹ *Dipartimento di Fisica e Astronomia, Università di Catania, Viale Andrea Doria 6, 95125 Catania, Italy*

² *International Institute of Physics, Universidade Federal do Rio Grande do Norte, 59012-970 Natal, Brazil*

Received: 2014 April 10; accepted: 2014 May 13

Abstract. We study through a semi-analytic model how the inner slopes of relaxed Λ CDM dark matter halos with and without baryons depend on the halo mass. We find that the inner logarithmic density slope, $\alpha \equiv d \log \rho / d \log r$, of dark matter halos with baryons has a significant dependence on the halo mass with slopes ranging from $\alpha \simeq 0$ for dwarf galaxies to $\simeq 1$ for clusters of galaxies. In the case of density profiles constituted just of dark matter, the mass dependence of slope is very slight. In the presence of baryons, the universality of the dark matter density profiles is no longer valid, in agreement with the results of several other authors, including the recent Di Cintio et al. (2014) simulations.

Key words: cosmology: theory – large-scale structure of Universe – galaxies: formation

1. INTRODUCTION

The Λ CDM model, although highly successful in describing the large-scale structure and evolution of the universe (Spergel et al. 2003; Komatsu et al. 2011; Del Popolo 2007, 2013, 2014), retains some problems in describing structures at small scales (e.g., Moore 1994; Moore et al. 1999; Ostriker & Steinhardt 2003; Boylan-Kolchin et al. 2011, 2012; Oh et al. 2011)¹. A noteworthy discrepancy is that between the cuspy density profiles of dark matter (DM) halos obtained in simulations (e.g., Navarro, Frenk & White 1996; 1997; Navarro 2010), and the flat density profiles of dwarf galaxies and LSBs (Low Surface Brightness galaxies) (Burkert 1995; de Blok et al. 2003; Del Popolo 2009 (DP09); Del Popolo & Kroupa (2009); Del Popolo 2012a,b (DP12a, DP12b); Del Popolo, Cardone & Belvedere 2013; Cardone & Del Popolo 2012; Cardone et al. 2011; Del Popolo & Hiotelis 2014; Oh et al. 2010, 2011; Kuzio de Naray & Kaufmann 2011). This discrepancy

¹ Other remaining problems for the Λ CDM model involve understanding dark energy: the cosmological constant fine tuning problem (Weinberg 1989; Astashenok & Del Popolo 2012), and the “cosmic coincidence problem”.

is known as Cusp/Core problem (see de Blok 2010).

A fundamental idea that has come out of the numerical approach is that relaxed halos are (nearly) universal in many respects: the phase-space density profile (Taylor & Navarro 2001), the linear relation between the density slope and the velocity anisotropy (Hansen & Moore 2006), the density profile (Navarro, Frenk & White 1996, hereafter NFW), the distribution of axial ratio, the distribution of spin parameter, and the distribution of internal specific angular momentum (Wang & White 2008).

The universal shape of the profiles, found by Navarro et al. (1996, 1997), has been confirmed by several other studies, even if the actual value of the inner density slope α has been a matter of controversy (Moore et al. 1998; Jing & Suto 2000; Ghigna et al. 2000; Fukushige & Makino 2001). More recently, the functional form of the universal profile has been substituted by the profiles whose logarithmic slope becomes increasingly shallower inwards (Power et al. 2003; Hayashi et al. 2004; Fukushige et al. 2004; Navarro et al. 2004; Stadel et al. 2009).

Moreover, there is also discussion whether the inner slope is actually universal or not (Moore et al. 1998; Jing & Suto 2000; Subramanian et al. 2000; Klypin et al. 2001; Ricotti 2003; Ricotti & Wilkinson 2004; Cen et al. 2004; Navarro et al. 2004; Fukushige et al. 2004; Merrit et al. 2005; Merrit et al. 2006; Graham et al. 2006; Ricotti et al. 2007; Gao et al. 2008; Host & Hansen 2011; Cardone, Leubner & Del Popolo 2011; Del Popolo 2011).

All of the previously quoted analyses dealing with universality of dark matter profiles do not study the possible effects produced by the presence of baryons, whose effect is to shallow (El-Zant et al. 2001, 2004; Romano-Diaz et al. 2008) and to steepen (Blumenthal et al. 1986; Gnedin et al. 2004; Klypin et al. 2002) the dark matter profile. In real galaxies, the two quoted effects combine, with the result of giving rise to density profiles which are different from those predicted in N-body simulations (Del Popolo 2009). In collisionless N-body simulations, this complicated interplay between baryons and dark matter is not taken into account, because it is very hard to include the effects of baryons in the simulations.

Recently, Di Cintio et al (2014) found, using Smooth Particle Hydrodynamics (SPH) simulations, that the inner density profiles of structures depend on the stellar mass and the halo mass. The main effect in their simulations, breaking the universality of the DM halo density profiles, is connected to the supernovae feedback: supernovae explode expelling baryonic matter from the structure. This produce a decrease of the central potential in the structure and the motion of DM particles toward the external parts of the halo, with a resulting flattening of the inner density profile. This is one of the proposed solutions to the Cusp/Core problem (Navarro et al. 1996; Gelato & Sommer-Larsen 1999; Read & Gilmore 2005; Mashchenko et al. 2006, 2008; Governato et al. 2010).

In the present paper, we study how baryons change the structure density profiles, by means of another model also used to solve the Cusp/Core problem, namely the angular momentum transfer from baryons to DM through dynamical friction (DF) (e.g., El-Zant et al. 2001, 2004; Romano-Diaz et al. 2008, 2009; Del Popolo 2009; Cole et al. 2011).

In the next sections, we use Del Popolo (2009) model to study how the inner slopes in density profiles change when baryons are present. The paper is organized as follows: in Section 2 we describe the Del Popolo (2009) model. In Section 3, we discuss the results. Finally, Section 4 is devoted to conclusions.

2. THE MODEL

In this section, we shortly summarize the model that will be used to study the behavior of the inner parts of the dark matter halos when baryons are present. The model was already discussed in Del Popolo (2009, DP09).

The model is an extension of the secondary infall model (SIM) (Gunn & Gott 1972; Fillmore & Goldreich 1984; Bertschinger 1985; Hoffman & Shaham 1985; Ryden & Gunn 1987; Henriksen & Widrow 1995, 1997, 1999; Henriksen & Le Delliou 2002; Le Delliou & Henriksen 2003; Le Delliou 2008; Ascasibar et al. 2004; Williams et al. 2004; Le Delliou et al. 2010, 2011a,b; Del Popolo, Pace & Lima 2013a,b; Del Popolo, Pace, Maydanyuk et al. 2013).

In the seminal paper of Gunn & Gott (1972), a bound mass shell of initial comoving radius x_i will expand to a maximum radius x_m (named apapsis or turnaround radius x_{ta}). As successive shells expand to their maximum radius, they acquire angular momentum and then contract on orbits determined by the angular momentum. Dissipative physics and the process of violent relaxation will eventually intervene and convert the kinetic energy of collapse into random motions (virialization).

The final density profile can be obtained in terms of the density at turn-around, $\rho_{ta}(x_m)$, the collapse factor², and the turn-around radius (Eq. A18, Del Popolo 2009), as:

$$\rho(x) = \frac{\rho_{ta}(x_m)}{f^3} \left[1 + \frac{d \ln f}{d \ln x_m} \right]^{-1} \quad (1)$$

In our model, proto-structures are formed around the peaks of the density field. In the calculation, we took into account the presence of baryons, their adiabatic collapse, dynamical friction and angular momentum. These quantities will be described below.

The density profile of a proto-halo is taken to be the profile of a peak in a density field described by the Bardeen et al. (1986) power spectrum, as is illustrated in Del Popolo (2009), Figure 6.

In the present paper, we take into account the ordered angular momentum, h , (Ryden & Gunn 1987, hereafter RG87) which arises from tidal torques experienced by proto-halos, and the random angular momentum, j , (RG87) which is connected to random velocities. Ordered angular momentum is got obtaining, first, the rms torque, $\tau(x)$, on a mass shell, then obtaining total specific angular momentum, $h(r, \nu)$, acquired during expansion by integrating the torque over time (Ryden 1988a (hereafter R88, Eq. 35), see Appendix C of Del Popolo (2009)).

The random part of the angular momentum was assigned to proto-structures according to Avila-Reese et al. (1998) scheme. This consists in expressing the specific angular momentum j through the ratio $e_0 = \left(\frac{r_{\min}}{r_{\max}} \right)_0$, where r_{\min} and r_{\max} are the maximum and minimum penetration of the shell toward the center, respectively, and left this quantity as a free parameter (see Appendix C of Del Popolo 2009).

In the present paper, we took into account dynamical friction by introducing the dynamical friction force in the equation of motion, see Del Popolo (2009), Eq. A16. Dynamical friction force was calculated dividing the gravitational field

² The collapse factor is defined as the $f = x/x_m$ (see Del Popolo 2009, Appendix A)

into an average and a random component generated by the clumps constituting hierarchical universes following Kandrup (1980), see Appendix D of Del Popolo (2009).

The shape of the central density profile is influenced by baryonic collapse: baryons drag dark matter in the so-called adiabatic contraction (AC) steepening the dark matter density slope.

The adiabatic contraction was taken into account by means of Gnedin et al. (2004) model and Klypin et al. (2002) model taking also account the exchange of angular momentum between baryons and dark matter (see appendix E of Del Popolo 2009 for a wider description). Our method of halo formation has considerable flexibility with direct control over the parameter space of initial conditions differently from numerical simulations which yield little physical insight beyond empirical findings precisely because they are so rich in dynamical processes, which are hard to disentangle and interpret in terms of underlying physics.

3. RESULTS AND DISCUSSION

3.1. Mass dependence of the inner slope

After describing the main points of the model, fully described in Del Popolo (2009), we will use it to determine the inner density slope of density profiles generated by the model. We calculate the logarithmic slopes, $\alpha \equiv d \log \rho / d \log r$, of the Λ CDM halos for different values of the mass at the radius $\sim 10^{-2} r_{\text{vir}}$ for three different cases: in the case A we take into account all the effects included in Del Popolo (2009), namely angular momentum, dynamical friction, baryons, baryon adiabatic contraction; in the case B there are no baryons and dynamical friction, and the angular momentum is taken into account as in Del Popolo (2009); in case C only angular momentum is taken into account reduced, as in Del Popolo (2009), in order to reproduce the angular momentum of N-body simulations (dashed line in Fig. 1) and a NFW profile (solid histogram in Fig. 1). We recall that in Del Popolo (2009), we performed an experiment similar to that performed by Williams et al. (2004), namely, we reduced the magnitude of the h and j angular momentum by a factor of 2, and the dynamical friction force by a factor of 2.5 with respect to the typical values calculated and used in the model in order to reproduce angular momentum of N-body simulations and the NFW profile.

Fig. 1 shows that the lower histogram representing the total specific angular momentum distribution of the density profile reproducing the NFW halo (described in the previously quoted experiment) is more centrally concentrated than the total specific angular momentum distribution of our reference halos (upper histogram), and is closer to those of typical halos emerging from numerical simulations. The dotted-dashed and dashed lines represent the quoted distribution of van den Bosch et al. (2002) for the halo versions 170 and 081, respectively. The halo ‘170’ resembles most to the specific angular momentum distributions, while the halo ‘081’ has the most shallow distribution in their simulations. This may suggest, in agreement with Williams et al. (2004), that halos in N-body simulations lose a considerable amount of angular momentum between 0.1 and $1 r_v$. Since virialization proceeds from inside out, this means that the angular momentum loss takes place during the later stages of the halo evolution, rather than on early stages. This is somehow confirmed by the so-called angular momentum catastrophe, namely the fact that the dark matter halos generated through

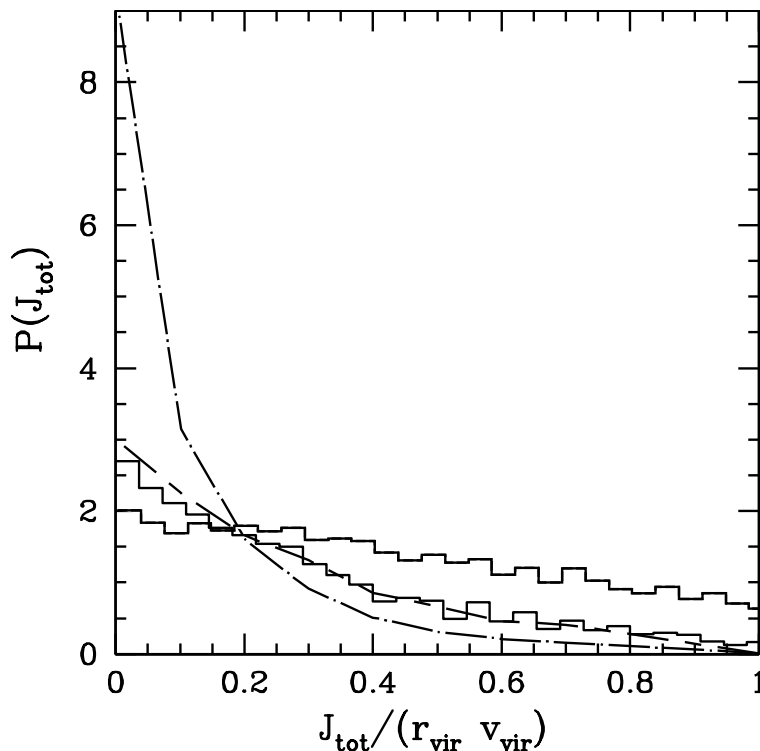


Fig. 1. Distribution of the total specific angular momentum, J_{tot} . The dotted-dashed and dashed lines represent the quoted distribution for the van den Bosch et al. (2002) halo versions 170 and 081, respectively. The upper histogram is the distribution obtained from our model for the $10^{12} M_{\odot}$ halo and the bottom histogram is the angular momentum distribution for the density profile reproducing the NFW halo, as described in the text.

gas-dynamical simulations are too small and have too little angular momentum compared to the halos of real disk galaxies, possibly because it was lost during repeated collisions through dynamical friction or other mechanisms (van den Bosch et al. 2002; Navarro & Steinmetz 2000). The problem can be solved invoking stellar feedback processes (Weil et al. 1998), but part of the angular momentum problem seems to originate due to numerical effects, most likely related to the shock capturing, artificial viscosity used in the smoothed particle hydrodynamic (SPH) simulations (Sommer-Larsen & Dolgov 2001).

The density profiles in Del Popolo (2009) (as in Williams et al. 2004) are shallower than N-body profiles. By reducing the amplitude of the angular momentum, the profiles get steeper at the center and one can find a value of angular momentum for which the NFW profile is reproduced, corresponding to the angular momentum seen in N-body simulations (solid line in Fig. 3). This effect can be understood as follows: the central density is built up by shells whose pericenters are very close to the center of the halo. Particles with larger angular momenta are prevented from coming close to the halo's center and so contributing to the central density. The correlation between increasing angular momentum and the reduction of inner slopes in halos has been also noticed by several other authors (Avila-Reese

et al. 1998, 2001; Subramanian et al. 2000; Nusser 2001; Hiotelis 2002; Le Delliou & Henriksen 2003; Ascasibar et al. 2003; Colafrancesco, Antonuccio-Delogu, Del Popolo 1995).

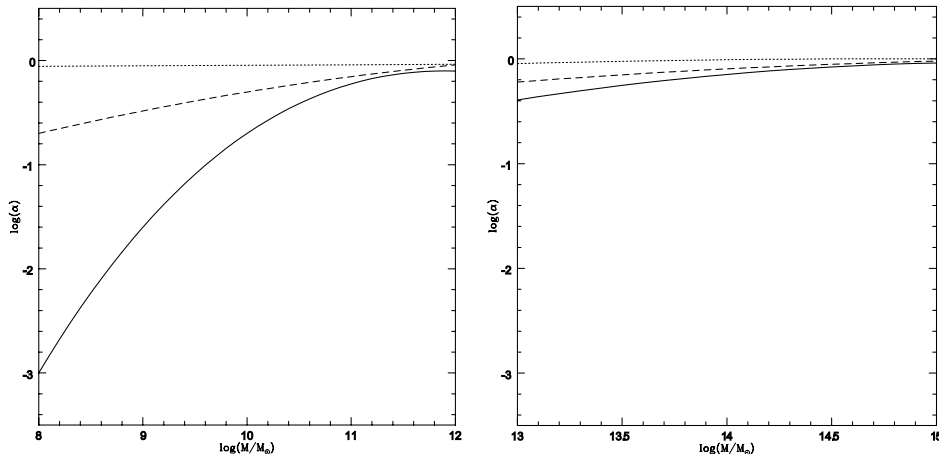


Fig. 2. The inner density slope as a function of halo mass. Panel (a): the solid, dashed and dotted lines represent the results of the model of the present paper for the cases A, B and C described in the text. Panel (b): the same as in (a) but for groups and clusters of galaxies.

In Fig. 2 we plot α , at $z = 0$, in terms of the mass for galaxies in the mass range $10^8 - 10^{12} M_\odot$. The solid, dashed and dotted lines represent: (a) the slope in the case A; (b) the slope in the case B; (c) the slope in the case C. The solid line (case A) shows that the inner profiles of dwarf galaxies are very flat with logarithmic slope $\alpha \simeq 0$ for $10^8 - 10^9 M_\odot$. Our results show a steepening of the density profile with increasing mass with the slopes $\alpha \simeq 0.2$ for $M \simeq 10^{10} M_\odot$, $\alpha \simeq 0.6$ for $M \simeq 10^{11} M_\odot$, $\alpha \simeq 0.8$ for $M \simeq 10^{12} M_\odot$. If we do not take into account baryons and dynamical friction (case B, dashed line), the shape of the density profiles becomes steeper with respect to case A, and the inner slopes are $\alpha \simeq 0.2$ for $M \simeq 10^8 M_\odot$, $\alpha \simeq 0.33$ for $M \simeq 10^9 M_\odot$, $\alpha \simeq 0.5$ for $M \simeq 10^{10} M_\odot$, $\alpha \simeq 0.7$ for $M \simeq 10^{11} M_\odot$, and $\alpha \simeq 0.91$ for $M \simeq 10^{12} M_\odot$. In the last case, the dotted line represents the quoted case C, and the profiles are even steeper than in the previous case B, and the inner slopes are $\alpha \simeq 0.88$ for $M \simeq 10^8 M_\odot$, $\alpha \simeq 0.90$ for $M \simeq 10^9 M_\odot$, $\alpha \simeq 0.91$ for $M \simeq 10^{10} M_\odot$, $\alpha \simeq 0.92$ for $M \simeq 10^{11} M_\odot$, and $\alpha \simeq 0.93$ for $M \simeq 10^{12} M_\odot$. The differences in the slopes with mass for the three plotted cases (A, B and C) can be explained as follows. In the case A (solid line), baryons, dynamical friction and angular momentum are present. The final density profile and the final slope is determined by the interplay of these three factors. Let us see how each of these factors act in shaping the profile and how they interplay. What concerns the angular momentum, we have to note that less massive objects are generated by peaks of smaller ν , which acquire more angular momentum (h and j) (Del Popolo & Gambera 1996).

The angular momentum sets the shape of the density profile at the inner regions. For pure radial orbits, the core is dominated by particles from the outer shells. As the angular momentum increases, these particles remain closer to the maximum radius, resulting in a shallower density profile. Particles with smaller an-

gular momentum will be able to enter the core but with a reduced radial velocity compared with the purely radial SIM. For some particles, the angular momentum is so large that they will never become unbound. Summarizing, particles of larger angular momenta are prevented from coming close to the halo centers and so contributing to the central density, which has the effect of flattening the density profile. The effects of dynamical friction can be interpreted in two different fashions: (a) an increase in dynamical friction force is very similar to changing the magnitude of angular momentum (see Fig. 11 of Del Popolo 2009) with the final result of producing shallower profiles; (b) dynamical friction can act on gas moving in the background of dark matter particles, dissipate the clump orbital energy and deposit it in the dark matter with the final effect of erasing the cusp (similarly to El-Zant et al. 2001, hereafter EZ01; El-Zant et al. 2004; Tonini, Lapi & Salucci 2006 (hereafter TLS); Romano-Diaz et al. 2008; Hiotelis & Del Popolo 2013). Baryons have another effect: at an early redshift, the dark matter density experiences the adiabatic contraction by baryons producing a slightly more cuspy profile. This last is overcome by the previous two effects. As shown by Fig. 11 of Del Popolo (2009), the magnitude of the dynamical friction effect is a bit larger than that due to the angular momentum and that these two effects add to improve the flattening of the profile. The quoted effects act in a complicated interplay. Initially, at high redshift (e.g., $z = 50$), the density profile is in the linear regime. The profile evolves to the non-linear regime and virializes. At an early redshift (e.g. $z \simeq 5$ for dwarf galaxies), the dark matter density experiences the adiabatic contraction by baryons producing a slightly more cuspy profile. The evolution after virialization is produced by a secondary infall, two-body relaxation, dynamical friction and angular momentum. Angular momentum, as described, contributes to reduce the inner slope of density profiles by preventing particles from reaching halo centers, while the dynamical friction dissipates the clump orbital energy and deposits it in the dark matter with the final effect of erasing the cusp (similarly to EZ01; El-Zant et al. 2004; TLS; Romano-Diaz et al. 2008). The cusp is slowly eliminated and within $\simeq 1$ kpc a core forms for objects with masses of dwarf-galaxies.

It is now clear why going from a model which takes into account baryons, dynamical friction, and angular momentum to a model taking account just the angular momentum or to a model taking account just the angular momentum reduced to reobtain N-body simulations of the angular momentum, larger inner slopes are obtained.

In Fig. 2b we plot the logarithmic slope in the case of groups and clusters of galaxies, similarly to Fig. 2a. The change of the slope with mass is qualitatively similar to the case of galaxies. However, in the case of groups and clusters the profiles are steeper showing a larger value of α . We obtain the following results: for masses $M \simeq 10^{13} M_\odot$, $M \simeq 10^{14} M_\odot$, $M \simeq 10^{15} M_\odot$ we have $\alpha \simeq 0.4, 0.6, 0.94$, respectively for the case A. For the case B the slopes are $\alpha \simeq 0.6, 0.8, 0.95$, and for the case C, $\alpha \simeq 0.96, 0.98, 1$.

The main reason of the difference in behavior between groups-clusters and galaxies is due to the fact that in the case of clusters the virialization process starts much later than to galaxies. In the case of galaxies the profile strongly evolves after virialization through the processes previously described. According to Del Popolo (2009), in the case of dwarf galaxies with $10^9 M_\odot$ the profile virializes at $z \simeq 10$, and from this redshift to $z = 0$ its shape continues to evolve. In the

case of a cluster of $10^{14} M_{\odot}$, the profile virializes at $z \simeq 0$ (Del Popolo 2009) and, as a consequence, the further evolution observed in galaxies cannot be observed in clusters.

It is evident from Fig. 2a and b that the inner slope of density profiles of dark matter and baryons (case A) and density profiles of dark matter characterized by standard angular momentum (case B) depends on mass. This result argues against the universality of this kind of profiles.

As previously reported, the dependence of the inner slope with mass has been observed in several N-body simulations (e.g. Navarro et al. 2004) and has received different interpretations. Gao et al. (2008) used two very large cosmological simulations to study how the density profiles of relaxed Λ CDM dark halos depend on redshift and on halo mass. The profiles obtained deviate slightly but systematically from the NFW form and are better approximated by the Einasto profile (Einasto 1965). They found that the shape parameter of the quoted profile changes with mass and redshift (see their Fig. 2). However, they interpret the result as supporting the idea that halo densities reflect the density of the universe at the time they formed, as proposed by Navarro et al. (1997). From this point of view, the shape parameter, α , should be used to improve the description of the typical density profiles of simulated halos and to eliminate possible biases in estimates of their concentration. Similarly Navarro et al. (2004) and Klypin et al. (2001) interpret the change in the value of the slope as a reflection of the trend between the concentration of the halo and its mass. Other studies, namely Merrit et al. (2005, 2006) interpret the systematic variation in profile shape with halo mass, as indicating that Λ CDM halos have not a truly universal profile, in agreement with previously quoted studies (Jing & Suto 2000; Subramanian et al. 2000; Ricotti 2003, Ricotti & Wilkinson 2004; Cen et al. 2004; Merrit et al. 2005; Ricotti et al. 2007; Host & Hansen 2009).

We should stress that in the case of DM N-body simulations the deviations from the NFW are slight, and for this reason one can arrive to different interpretations and try to reduce the discrepancy by modifying the definition of halo formation time, the concentration vs. mass relation, as in Gao et al. (2008).³ In our case A, density profiles have a final shape highly different from that of a NFW density profile or its improvements (e.g., Navarro et al. 2004), since our profiles contain not only DM but also baryons. For this reason, a comparison of our result for the case A with previous ones, is not easy since all previous studies finding or not, a universal behavior in density profiles, are dealing just with DM halos: they do not take account the effect of baryons. In the case A of our model there is no room for different interpretations as in previous studies: the density profiles are so different from those obtained in N-body simulations, and the inner slopes changes so strongly with mass that we are compelled to the conclusion that when baryons are taken into account the profiles are not universal.

Similar conclusions are valid for the case B: the mass dependence of the inner slope, $\alpha(M)$, is so strong that it leads to the conclusion that the profiles in this case are not universal too.

In the case C the mass dependence of the slope is quite small. This means that in the case of a DM proto-structure with angular momentum reduced to reproduce angular momentum in N-body simulations (dashed line or solid histogram in Fig.

³ Even with the quoted interpretation, the evolution of the concentrations of the Milky Way mass halos is still not reproduced well.

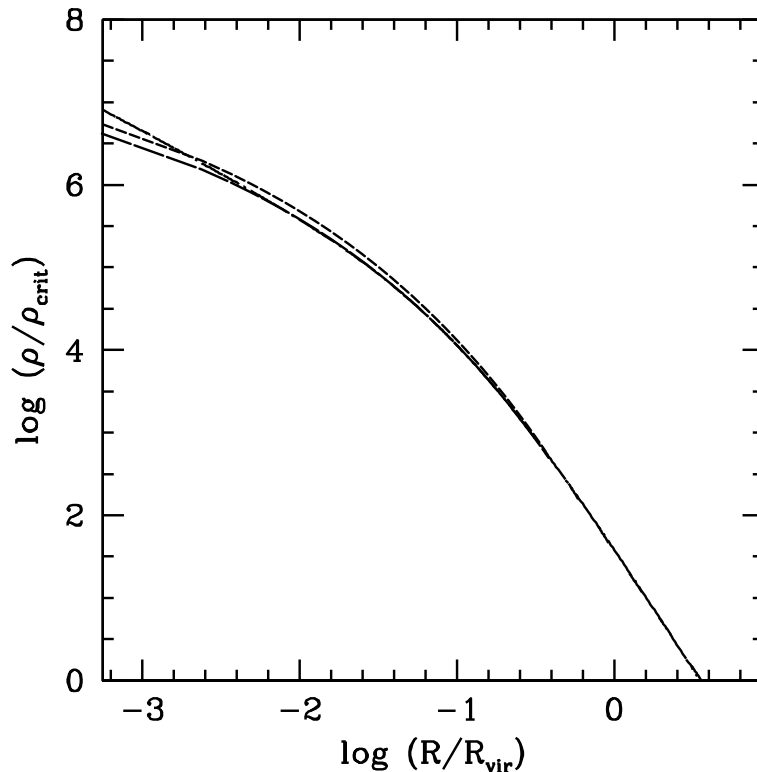


Fig. 3. Comparison of halos generated by the model of the present paper (long-dashed line) with the numerical simulations. The solid line is the NFW profile while the short-dashed line is the result of the Aquarius experiment, both for a halo with $10^{12} M_{\odot}$.

1) the density profiles and slopes have a similar behavior to those obtained in N-body simulations. In this case the slight slope change with mass could be interpreted as in Merrit et al. (2006) or differently as in Navarro et al. (2004) and Klypin et al. (2001). However, even following the interpretation of Navarro et al. (2004), who wrote “adjusting the parameter n allows the profile to be tailored to each individual halo, resulting in improved fits”⁴, such a breaking of structural homology (see Graham & Colless 1997 for an analogy with the projected luminosity profiles) replaces the notion that a universal density profile may exist.

Finally, we checked if the model of the present paper gives the results in agreement with dissipationless simulations, when baryons are not taken into account and the angular momentum is fixed as in Fig. 1 (dashed line). In Fig. 3 we plot the profiles obtained with our model and those predicted by the numerical simulations. The long-dashed line represents the density profile for halos with $10^{12} h^{-1} M_{\odot}$. In order to compare the results of the model with those of N-body simulations, we plot the NFW profile (solid line) for halos with masses equal to $10^{12} h^{-1} M_{\odot}$, and the results for the same mass obtained in the Aquarius Project

⁴ The value of n , equal to $1/\alpha$ in the Navarro et al. (2004) notation, ranged from 4.6 to 8.2 (Table 3 in Navarro et al.).

by Navarro et al. (2010) (short-dashed line). The plot shows that the result of the present paper is in good agreement with simulations and similarly to Navarro et al. (2010) the density profiles deviate slightly but systematically from the NFW model, and are approximated more accurately by the Einasto profile. Density profiles become monotonically shallower inwards, down to the innermost resolved point, with no indication that they approach power-law behavior. The innermost slope is slightly shallower than -1 . Shallower cusps, such as the $r^{-0.75}$ behavior predicted by the model of Taylor & Navarro (2001), cannot yet be excluded.

3.2. Comparison with other studies

A comparison of the present results, concerning the density profile shape and inner slopes, with other studies has somehow already been performed in Del Popolo (2009).

The results of the case A agree with those of Romano-Diaz et al. (2008) who studied the DM cusp evolution using N-body simulations with and without baryons. Their study shows how baryons tend to reduce the inner slope because of the heating up of the cusp region via dynamical friction (EZ01) or influx of subhalos into the innermost region of the DM halo. Our results are in agreement with EZ01 and El-Zant et al. (2004) arguing that dynamical friction acting on galaxies moving within the DM background opposes the effect of adiabatic compression by transferring their orbital energy to the DM, thus heating up and softening the inner profile. Moreover, our density profiles and inner slopes agree very well with Gentile et al. (2004) rotation curves of some LSB galaxies (Fig. 4 in Del Popolo 2009), and with several studies observing shallower inner slopes than simulations (Flores & Primack 1994; Moore 1994; Burkert 1995; Kravtsov et al. 1998; Salucci & Burkert 2000; Borriello & Salucci 2001; de Blok et al. 2001, 2003; de Blok & Bosma 2002; de Blok 2003; Spekkens et al. 2005). In the case of clusters, the results agree with observations finding non-cuspy profiles (e.g., Ettori et al. 2002; Sand et al. 2002, 2004).

A direct comparison of the result of our case A can be made with the results of Di Cintio et al. (2014). As already reported, the galaxies forming in their SPH simulations are strongly affected by supernovae feedback and the inner slope of the DM density profile depends on the mass. In Fig. 4, we compare our result for α with the result given in their Fig. 6. In Fig. 4 the red, blue and black lines represent the dependence of α on the circular velocity v_c in the three radial ranges: $3 < r/\epsilon < 10^5$, $1 < r/\text{kpc} < 2$, $0.01 < r/R_{\text{vir}} < 0.02$, respectively. The last is related to the virial mass by

$$v_c = 2.8 \times 10^{-2} M_{\text{vir}}^{0.316} \quad (2)$$

where the virial mass is expressed in units of $h^{-1} M_{\odot}$, and the circular velocity in km/s.

The dotted curve is the result of our calculation. The plot shows that our α vs. v_c relation is similar to that of Di Cintio et al. (2014) in the range 40–250 km/s. For $v_c < 40$ km/s our results predict galaxies with cored profiles, while Di Cintio et al. (2014) results show a steepening of the profile which has $\alpha \simeq -1.2$ around 5 km/s. A different behavior of the slope at small velocities could be used to discriminate among the models like ours, based on the interaction of baryons

⁵ ϵ is the softening length of each galaxy.

and DM through dynamical friction, and the models like that of Di Cintio et al. (2014) based on the supernovae feedback mechanism. We will focus on this issue in a next paper. In the present one, we want to recall that some of the Milky Way dSphs (e.g., Fornax, Sculptor) point towards cored profiles (Goerdt et al. 2006; Battaglia et al. 2008; Walker & Peñarrubia 2011; Amorisco & Evans 2012; Agnello & Evans 2012; Cole et al. 2012; Jardel & Gebhardt 2012; Jardel et al. 2013; Jardel & Gebhardt 2013; Breddels et al. 2013; Lora et al. 2013), in agreement with our result.

Considering the case B, our results agree with all listed studies showing that the higher is the value of angular momentum, the flatter is its inner slope (e.g., Avila-Reese et al. 1998; Nusser 2001; Hiotelis 2002; Le Delliou & Henriksen 2003; Williams et al. 2004). The case C, as described above, gives the inner slopes similar to those obtained in N-body simulations (e.g., Navarro et al. 2004).

A comparison of our results concerning the universality of density profiles with other studies is more problematic, especially in the case of dissipationless N-body simulations which do not take account of baryons.

In the case A, our results are in agreement with those studies that have argued against the quoted universality in DM simulations (Jing & Suto 2000; Subramanian et al. 2000; Ricotti 2003; Ricotti & Wilkinson 2004; Cen et al. 2004; Graham et al. 2006; Merrit et al. 2005; Ricotti et al. 2007). Our result also agrees with observational evidences of non-universality in dark matter density profiles both in galaxy scale (Simon et al. 2003, 2004a,b) and in cluster scales (Host & Hansen 2009). Similar conclusions are valid for the case B. Considering the case C, our result is in agreement with Merrit et al. (2006) which concludes that there is a significant mass dependence in the density profiles of halos.

In the case C, to better explore how the homology (i.e., universality) of CDM halos is broken, it would be important to analyze a large, low-resolution sample of halos from a cosmological cube simulation, in order to obtain good statistics. Moreover, the presence of large subhalos, possible debris wakes from larger structures and the collective impact from differing degrees of virialization in the outer regions could be quantified.

4. CONCLUSIONS

In the present paper, we studied the dependence of the inner slope of the density profiles of dark matter halos with and without baryons. The density profiles were constructed using the Del Popolo (2009) method, which includes the effect of baryons on dark matter halos. We calculated the inner slopes for the three different cases: in the case A we take into account all the effects included in Del Popolo (2009), namely angular momentum, dynamical friction, baryons and baryon adiabatic contraction; in the case B baryons and dynamical friction are missing, and the angular momentum is taken into account as in Del Popolo (2009); in the case C only the angular momentum is taken into account with magnitude reduced comparing to Del Popolo (2009) in order to reproduce the angular momentum of N-body simulations. In the cases A and B we found a strong dependence of the inner slope on the mass: lower mass objects have smaller slopes. This result argues against the universality of profiles of this type. When baryons are not present (the case C), the mass dependence of slope is quite small, in agreement with the results of other studies (e.g., Gao et al. 2008).

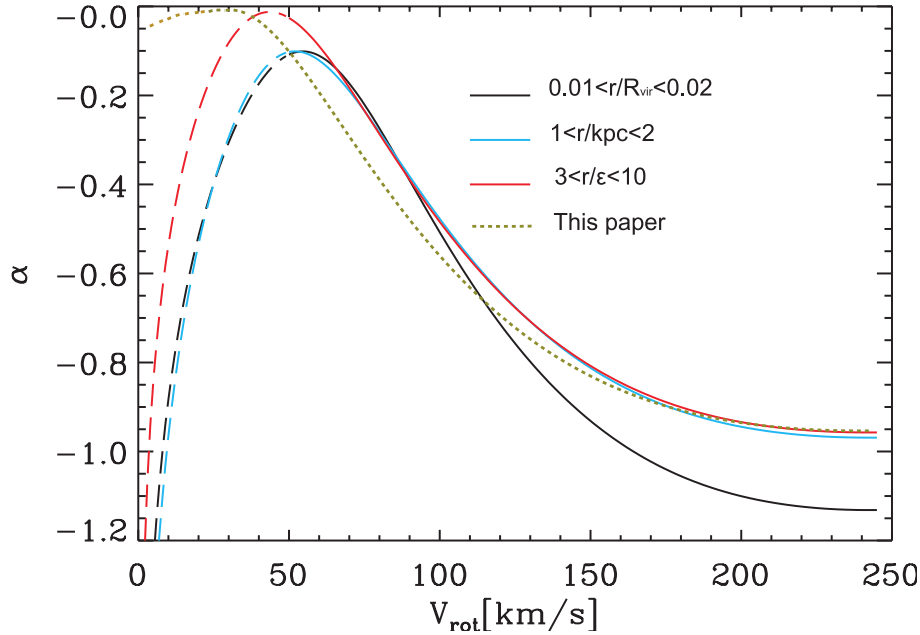


Fig. 4. The α vs. v_c relation. The three continuous lines represent the result of Di Cintio et al. (2014) in three radial ranges, and the dotted line is our result. The dashed lines in the left side of their maxima are extrapolations of the baryonic TF relation (Dutton et al. 2010) for stellar mass smaller than $10^9 M_\odot$.

The mass dependence of the inner slope, and the consequent non-universality of the DM density profiles, coming out from our results, is in agreement with several previous results and with recent SPH simulations of Di Cintio et al. (2014).

ACKNOWLEDGMENTS. I thank Professor B. Moore for some helpful suggestions.

REFERENCES

- Agnello A., Evans N. W. 2012, *ApJ*, 754, L39
 Amorisco N. C., Evans N. W. 2012, *MNRAS*, 419, 184
 Ascasibar Y., Yepes G., Göttlober S., Müller V. 2004, *MNRAS*, 352, 1109A
 Astashenok A. V., Del Popolo, A. 2012, *Class. Quant. Grav.*, 29, 085014 [arXiv:1203.2290]
 Avila-Reese V., Colin P., Valenzuela O. et al. 2001, *ApJ*, 559, 516
 Avila-Reese V., Firmani C., Hernandez X. 1998, *ApJ*, 505, 37
 Bardeen J. M., Bond J. M., Kaiser N., Szalay A. S. 1986, *ApJ*, 304, 15
 Battaglia G., Helmi A., Tolstoy E. et al. 2008, *ApJ*, 681, L13
 Bertschinger E. 1985, *ApJS*, 58, 39
 Blumenthal G. R., Faber S. M., Flores R., Primack J. R. 1986, *ApJ*, 301, 27
 Borriello A., Salucci P. 2001, *MNRAS*, 323, 285
 Boylan-Kolchin M., Bullock J. S., Kaplinghat M. 2011, *MNRAS*, 415, L40
 Boylan-Kolchin M., Bullock J. S., Kaplinghat M. 2012, *MNRAS*, 422, 1203

- Breddels M. A., Helmi A., van den Bosch R. C. E. et al. 2013, MNRAS, 433, 3173
- Burkert A. 1995, ApJ, 447, L25
- Cardone V. F., Del Popolo A. 2012, MNRAS, 427, 3176
- Cardone V. F., Leubner M. P., Del Popolo A. 2011, MNRAS, 414, 2265
- Cardone V. F., Del Popolo A., Tortora C., Napolitano N. R. 2011, MNRAS, 416, 1822
- Cen R. Y., Dong F., Bode P., Ostriker J. P. 2004, ArXiv, astro-ph/0403352
- Colafrancesco S., Antonuccio-Delogu V., Del Popolo A. 1995, ApJ, 455, 32
- Cole D. R., Dehnen W., Wilkinson M. I. 2011, MNRAS, 416, 1118
- Cole D. R., Dehnen W., Read J. I., Wilkinson M. I. 2012, MNRAS, 426, 601
- de Blok W. J. G., McGaugh S. S., Bosma A., Rubin V. C. 2001a, ApJ, 552, L23
- de Blok W. J. G., McGaugh S. S., Rubin V. C. 2001b, AJ, 122, 2396
- de Blok W. J. G., Bosma A., McGaugh S. 2003, MNRAS, 340, 657
- de Blok W. J. G., Bosma A. 2002, A&A, 385, 816
- de Blok W. J. G. 2010, Advances in Astronomy, Volume 2010, ID 789293
- Del Popolo A. 2002, MNRAS, 337, 529
- Del Popolo A. 2007, Astron. Rep., 51, 169
- Del Popolo A. 2009, ApJ, 698, 2093
- Del Popolo A. 2011, JCAP, 07, 014
- Del Popolo A. 2012a, MNRAS, 424, 38
- Del Popolo A. 2012b, MNRAS 419, 971
- Del Popolo A. 2013, AIP Conf. Proc., 1548, 2
- Del Popolo A. 2014, Int. J. Mod. Phys. D, 23, 1430005
- Del Popolo A., Cardone V. F., Belvedere G. 2013, MNRAS, 429, 1080
- Del Popolo A., Gambera M. 1996, A&A, 308, 373
- Del Popolo A., Hiotelis N. 2014, JCAP, 01, 047
- Del Popolo A., Kroupa P. 2009, A&A, 502, 733
- Del Popolo A., Pace F., Lima J. A. S. 2013a, MNRAS, 430, 628
- Del Popolo A., Pace F., Lima J. A. S. 2013b, Int. J. Mod. Phys. D, 22, 1350038
- Del Popolo A., Pace F., Maydanyuk S. P. et al. 2013, Phys. Rev. D, 87, 043527
- Di Cintio A., Brook C. B., Macci A. V. et al. 2014, MNRAS, 437, 415
- Einasto J. 1965, Trudy Inst. Astrofiz. Alma-Ata, 5, 87
- El-Zant A., Hoffman Y., Primack J. et al. 2004, ApJ, 607, L75
- El-Zant A., Schlosman Y., Hoffman Y. 2001, ApJ, 560, 636 (EZ01)
- Ettori S., Fabian A. C., Allen S. W., Johnstone R. M. 2002, MNRAS, 331, 635
- Filmore J. A., Goldreich P., 1984, ApJ, 281, 1
- Flores R. A., Primack J. R. 1994, ApJ, 427, L1
- Fukushige T., Kawai A., Makino J. 2004, ApJ, 606, 625
- Fukushige T., Makino J. 2001, ApJ, 557, 533
- Gao L., Navarro J. F., Cole S. et al. 2008, MNRAS, 387, 536
- Gelato S., Sommer-Larsen J. 1999, MNRAS, 303, 321
- Gentile G., Salucci P., Klein U. et al. 2004, MNRAS, 351, 903
- Ghigna S., Moore B., Governato F. et al. 2000, ApJ, 544, 616
- Gnedin O. Y., Kravtsov A. V., Klypin A. A., Nagai D. 2004, ApJ, 616, 16
- Goerdt T., Moore B., Read J. I. et al. 2006, MNRAS, 368, 1073

- Governato F., Brook C. B., Brooks A. M. et al. 2010, *Nature*, 463, 203
- Graham A. W., Colless M. M. 1997, *MNRAS*, 287, 221
- Graham A. W., Merritt D., Moore B. et al. 2006, *AJ*, 132, 2701
- Gunn J. E. 1977, *ApJ*, 218, 592
- Gunn J. E., Gott J. R. 1972, *ApJ*, 176, 1
- Hayashi E., Navarro J. F., Power C. et al. 2004, *MNRAS*, 355, 794
- Henriksen R. N., Le Delliou M. 2002, *MNRAS*, 331, 423
- Hiotelis N. 2002, *A&A*, 383, 84
- Hiotelis N., Del Popolo A. 2013, *MNRAS*, 436, 163
- Hoffman Y., Shaham J. 1985, *ApJ*, 297, 16
- Host O., Hansen S. H. 2011, *ApJ*, 736, 52
- Jardel J. R., Gebhardt K. 2012, *ApJ*, 746, 89
- Jardel J. R., Gebhardt K., Fabricius M. H. et al. 2013, *ApJ*, 763, 91
- Jing Y. P., Suto Y. 2000, *ApJ*, 529, L69
- Kandrup H. E. 1980, *Phys. Rep.*, 63, no. 1, 1
- Klypin A., Zhao H., Somerville R. S. 2002, *ApJ*, 573, 597
- Klypin A., Kravtsov A. V., Bullock J. S. et al. 2001, *ApJ*, 554, 903
- Klypin A. A., Trujillo-Gomez S., Primack J. 2011, *ApJ*, 740, 102
- Komatsu E., Smith K. M., Dunkley J. et al. 2011, *ApJS*, 192, 18
- Kuzio de Naray R., Kaufmann T. 2011, *MNRAS*, 414, 3617
- Le Delliou M. 2008, *A&A*, 490, L43
- Le Delliou M., Henriksen R. N. 2003, *A&A*, 408, 27
- Le Delliou M., Henriksen R. N., MacMillan J. D. 2010, *A&A*, 522, A28
- Le Delliou M., Henriksen R. N., MacMillan J. D. 2011a, *A&A*, 526, A13
- Le Delliou M., Henriksen R. N., MacMillan J. D. 2011b, *MNRAS*, 413, 1633
- Lora V., Grebel E. K., Sanchez-Salcedo F. J. et al. 2013, *ApJ*, 777, 65
- Mashchenko S., Couchman H. M. P., Wadsley, J. 2006, *Nature*, 442, 539
- Mashchenko S., Wadsley J., Couchman H. M. P. 2008, *Science*, 319, 174
- Merritt D., Navarro J. F., Ludlow A., Jenkins A. 2005, *ApJ*, 624, L85
- Merritt D., Graham A. W., Moore B. et al. 2006, *AJ*, 132, 2685
- Moore B. 1994, *Nature*, 370, 629
- Moore B., Governato F., Quinn T., Stadel J. et al. 1998, *ApJ*, 499, L5
- Navarro J. F., Steinmetz M. 2000, *ApJ*, 538, 477
- Navarro J. F., Frenk C. S., White S. D. M. 1996, *ApJ*, 462, 563
- Navarro J. F., Frenk C. S., White S. D. M. 1997, *ApJ*, 490, 493
- Navarro J. F., Hayashi E., Power C. et al. 2004, *MNRAS*, 349, 1039
- Navarro J. F., Ludlow A., Springel V. et al. 2010, *MNRAS*, 402, 21
- Nusser A. 2001, *MNRAS*, 325, 1397
- Oh S.-H., de Blok W. J. G., Brinks E. et al. 2011, *AJ*, 141, 193
- Ostriker J. P., Steinhardt P. J. 2003, *Science*, 300, 1909
- Power C., Navarro J. F., Jenkins A. et al. 2003, *MNRAS*, 338, 14
- Read J. I., Gilmore G. 2005, *MNRAS*, 356, 107
- Ricotti M. 2003, *MNRAS*, 344, 1237
- Ricotti M., Pontzen A., Viel M. 2007, *ApJ*, 663, 53
- Ricotti M., Wilkinson M. I. 2004, *MNRAS*, 353, 867
- Romano-Diaz E., Shlosman I., Heller C., Hoffman Y. 2009, *ApJ*, 702, 1250

- Romano-Diaz E., Shlosman I., Hoffman Y., Heller C. 2008, ApJ, 685, L105
Ryden B. S., Gunn J. E. 1987, ApJ, 318, 15
Ryden B. S. 1988a, ApJ, 329, 589
Ryden B. S. 1988b, ApJ, 333, 78
Salucci P., Burkert A. 2000, ApJ, 537, L9
Sand D. J., Treu T., Ellis R. S. 2002, ApJ, 574, L129
Sand D. J., Treu T., Smith G. P., Ellis R. S. 2004, ApJ, 604, 88
Simon J. D., Bolatto A. D., Leroy A., Blitz L. 2003, ApJ, 596, 957
Simon J. D., Bolatto A. D., Leroy A., Blitz L. 2004a, in *Satellites and Tidal Streams*, ASPC, 327, 18
Simon J. D., Bolatto A. D., Leroy A., Blitz L., Gates E. L. 2004b, ApJ, 621, 757
Sommer-Larsen J., Dolgov A. 2001, ApJ, 551, 608
Spekkens K., Giovanelli R., Haynes M. P. 2005, AJ, 129, 2119
Spergel D. N., Verde L., Peiris H. V. et al. 2003, ApJS, 148, 175
Stadel J., Potter D., Moore B. et al. 2009, MNRAS, 398, L21
Stiavelli M., Miller B. W., Ferguson H. C. et al. 2001, AJ, 121, 1385
Subramanian K., Cen R., Ostriker J. P. 2000, ApJ, 538, 528
Taylor J. E., Navarro J. F. 2001, ApJ, 563, 483
Tonini C., Lapi A., Salucci P. 2006, ApJ, 649, 591
Toth G., Ostriker J. P. 1992, ApJ, 389, 5
van den Bosch F. C., Abel T., Croft R. A. C. et al. 2002, ApJ, 576, 21
Walker M. G., Peñarrubia J. 2011, ApJ, 742, 20
Weil M. L., Eke V. R., Efstathiou G. 1998, MNRAS, 300, 773
Weinberg S. 1989, Rev. Mod. Phys., 61, 1
Williams L. L. R., Babul A., Dalcanton J. J. 2004, ApJ, 604, 18